

Interaction of NO₂ with a Pt(111) Surface

J. SEGNER, W. VIELHABER AND G. ERTL

Institut für Physikalische Chemie, Universität München, 8 München 2, FRG

(Received 19 May 1982)

Abstract. The interaction of NO₂ with a Pt(111) surface was studied by molecular beam and thermal desorption techniques. At 300 K NO₂ adsorbs dissociatively into NO_{ad} + O_{ad} with an initial sticking coefficient $s_0 = 0.97$. s_0 decreases slightly with increasing surface temperature; the variation of the sticking coefficient with coverage exhibits a marked "precursor" state behavior. The rate of formation of gaseous NO is limited by desorption of this molecule, i.e. there is no evidence for a direct process NO₂ → NO_g + O_{ad}. At ≈ 400 K NO desorption is complete and only O_{ad} is building up on the surface. The maximum coverage $\theta_{0,\max} \approx 0.77$ is much higher than that so far reported for exposure to O₂ (0.25), which is ascribed to kinetic effects, i.e. a much higher sticking coefficient in the case of NO₂. Two additional states with desorption energies of about 32 and 38 kcal/mol characterize the high oxygen coverage situation. Desorption of O₂ starts above 450 K.

1. INTRODUCTION

Despite its importance in catalytic air pollution control, systematic investigations on the interaction of NO₂ with well-defined single crystal surfaces of the platinum group metals are so far missing. The present work is the first report on such a system in which the interaction between NO₂ and a Pt(111) surface was studied by means of molecular beam and thermal desorption techniques. This continues previous studies with the same methods and surface on the interaction of CO,¹ O₂,² and NO,³ as well as on the catalytic oxidation of CO.⁴

2. EXPERIMENTAL

Details of the molecular beam apparatus have been described elsewhere.^{2,5} In brief, it consists of a three-stage differentially pumped nozzle beam source connected with the UHV chamber, in the center of which the sample was mounted on a manipulator. A quadrupole mass spectrometer 4 cm away from the sample can be rotated to vary the detection angle, and the sample can be rotated in order to vary the angle of incidence.

Preparation and characterisation of the Pt(111) surface is described in Ref. 2. NO₂ (purity 98%) was introduced through stainless-steel valves. The NO content of the beam may rise up to about a few percent by partial dissociation of NO₂ in the valves etc. Corrosion of the forepumps could be minimized by the use of a chemical oil filter (Balzers OFC 003).

3. RESULTS

3.1. Kinetics of Adsorption

If a clean Pt(111) surface is exposed at 300 K to a NO₂ beam, only about 3% of the incoming flux is scattered back. The major fraction being adsorbed never desorbs as NO₂, but only in the form of NO + O₂. This indicates very efficient dissociative adsorption, viz.



and a subsequent increase of the temperature causes recombination and desorption of oxygen ($2\text{O}_{\text{ad}} \rightarrow \text{O}_2$), as well as desorption of NO. UPS experiments at surface temperatures as low as 120 K revealed indeed no evidence for the existence of an NO_{2,ad}-species with appreciable concentration but indicated complete dissociation even at low temperatures.⁶ With increasing coverage the dissociative sticking coefficient of course decreases and

the flux of backscattered NO₂ increases. The angular distribution of these molecules follows the Knudsen (cosine) law, quite similar to the case of CO² or NO³ scattering. This effect has analogously to be attributed to a trapping/desorption mechanism for a short-lived "precursor" state of NO₂ molecules in a second layer on top of the chemisorbed phase which will be substantiated by the data on the variation of the (dissociative) sticking coefficient with coverage.

Since the angular distribution of reflected NO₂ molecules does not vary with coverage, the fraction of the primary flux being chemisorbed (= sticking coefficient) can easily be determined as a function of time by means of transient measurements^{5,7}: The mass spectrometer is kept at a fixed position and records the NO₂ partial pressure (which is proportional to the flux I of molecules coming off the surface) as a function of time after a constant primary flux I_0 is suddenly switched on at time t_0 (Fig. 1). $I(t)$ follows the dashed line, but would follow the full line if no adsorption were to take place. The sticking coefficient at time t is then simply given by

$$s(t) = 1 - I(t)/I_0, \quad (1)$$

i.e., no further calibration is needed. Transformation of the time scale into coverage, θ , or surface concentration, n_s , is straightforward in the case of a single component adsorbate once the primary flux is known, viz.

$$n_s = I_0 \int_0^t s(t) dt. \quad (2)$$

The situation is more complicated in the present case, where the total coverage is composed of fractional coverages,

$$\theta_{\text{tot}} = \theta_0 + \theta_{\text{NO}}.$$

Since NO starts to desorb already at 300 K,³ in general $\theta_0 \neq \theta_{\text{NO}}$. Procedures by which I_0 , θ_0 and θ_{NO} could be determined are outlined in the appendix. As an example, Fig. 2 shows the variation of θ_0 and θ_{NO} with NO₂ exposure (= time × NO₂ pressure) at a sample temperature of 303 K: At low coverages $\theta_0 = \theta_{\text{NO}}$ due to stoichiometry, but then θ_{NO} passes through a maximum while θ_0 increases continuously. This indicates that the

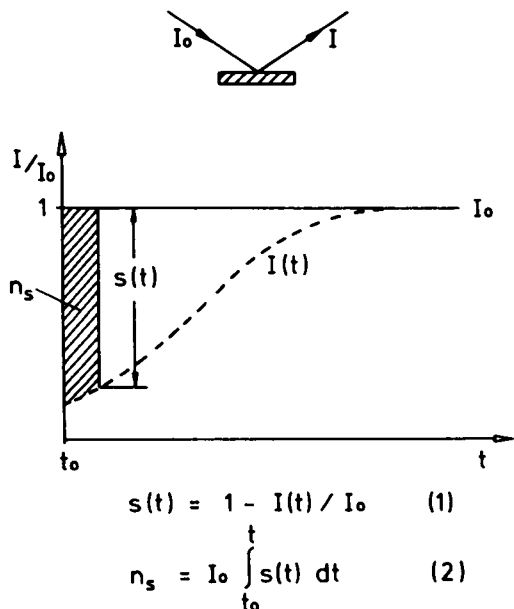


Fig. 1. Schematic illustration of the transient molecular beam technique.

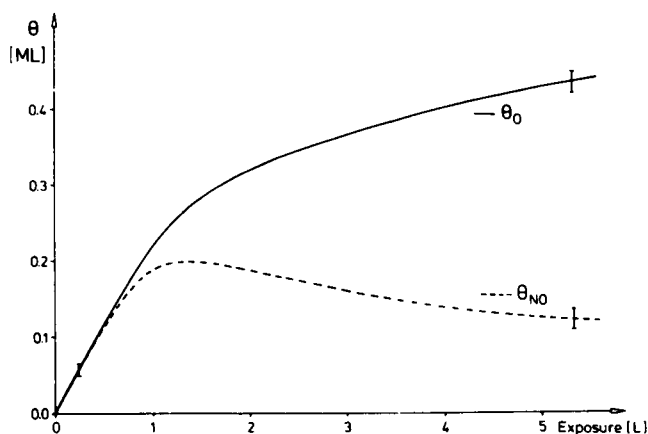


Fig. 2. Variation of the fractional NO- and O-coverages with NO_2 exposure at $T_s = 303$ K.

build-up of O_{ad} lowers the adsorption energy of NO so that desorption takes place, which is in complete agreement with previous studies on the coadsorption of O + NO.³ At temperatures ≥ 420 K the maximum NO-coverage will be negligibly small, while oxygen starts to desorb only above 450 K (see below).

Figure 3 shows the variation of the sticking coefficient with coverage at 298 K and 440 K sample temperatures. In the former case the adsorbed phase consists of both O_{ad} + NO_{ad} (compare with Fig. 2), while at the higher temperature $\theta_{\text{tot}} = \theta_0$ due to complete desorption of NO. It is surprising that in this way a maximum oxygen coverage of 0.77 ± 0.05 can be reached, while low pressure interaction with O_2 is terminated at $\theta_{0,\text{max}} = 0.25$.^{2,8,9} The variation of s with coverage is qualitatively quite similar to the findings with CO¹ or NO³ on Pt(111) and can again be ascribed to the existence of a precursor state: A NO_2 molecule striking an already occupied site

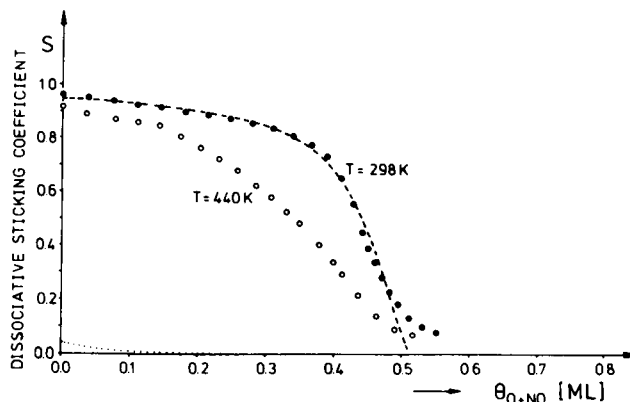


Fig. 3. Variation of the dissociative sticking coefficient with total coverage θ_{tot} at 298 K and 440 K. At 440 K $\theta_{\text{tot}} = \theta_0$. The dashed line represents the best fit of the data at 298 K with Eq. (3). Dotted line: $s(\theta) - \text{O}_2$ at 440 K.

on the surface is physisorbed there with a very high trapping probability and will now, via surface diffusion, probably find an empty site for dissociative chemisorption prior to desorption. The above-mentioned observation of a cosine angular distribution of backscattered NO_2 molecules at higher coverages is in full accord with this picture of a short-lived but thermally accommodated precursor state.

It is expected that the mathematical model for dissociative chemisorption via a precursor state, as developed by Kisliuk,¹⁰ will not provide a quantitative description of the present results since it does not include the possibility of desorption of part of the *chemisorbed* particles which, however, will be the case for NO, even at 300 K (cf. Fig. 2). In this model the sticking coefficient varies with the relative coverage $\vartheta = \theta/\theta_{\text{max}}$ according to

$$s = s_0 \cdot \frac{(1 - \vartheta)^2}{1 - \vartheta(1 - K) + \vartheta^2 s_0} \quad (3)$$

The dashed line in Fig. 3 gives the best fit with experimental data with parameters $K = -0.93$ and $\theta_{\text{max}} = 0.52$. The failure of the model becomes, however, evident if θ_{max} is considered which, in fact, is ~ 0.75 instead of 0.52, used as the parameter. Apart from non-negligible desorption, interactions between the adsorbed particles¹¹ would also have to be taken into account in order to obtain a more appropriate theoretical description at higher coverages.

The initial sticking coefficient is very high, e.g. $s_0 = 0.97$ at 300 K. This is indeed the highest value of a sticking coefficient for *dissociative* adsorption so far known to us. The variation of s_0 with surface temperature is reproduced in Fig. 4. The slight decrease with increasing T_s can be ascribed qualitatively to the increasing energy transfer from the vibrating surface atoms upon impact. Extrapolation of the data to lower temperatures suggests that s_0 may become very close to unity.

3.2. Desorption of Oxygen

Since O_2 desorbs at higher temperatures than NO ,^{2,3} no information on the influence of NO_{ad} on the desorption kinetics of oxygen can be obtained, but instead the data presented now are representative for pure O_{ad} -layers.

Thermal desorption spectra for O_2 were recorded with a heating rate of 8.6 K/s after exposing the surface at 440 K to various amounts of NO_2 . Data are reproduced in

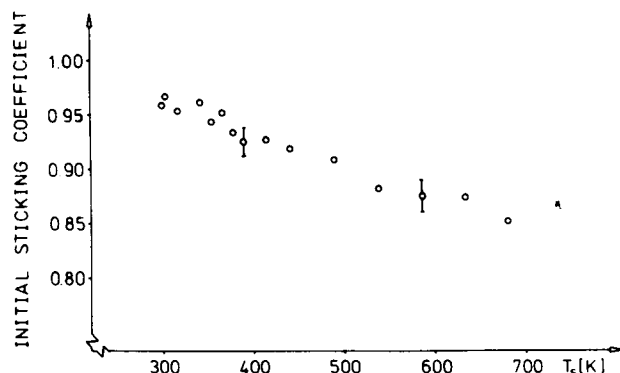


Fig. 4. Variation of the initial sticking coefficient with surface temperature T_s .

Fig. 5a and are characterized by three desorption states, β_1 , β_2 and β_3 , which are subsequently filled. The β_3 state is identical to the data obtained after exposure to O_2 shown in Fig. 5b which saturates at $\theta_0 = 0.25$.² The kinetics of desorption from this state have been analysed previously in terms of a second-order process with preexponential $\nu(\beta_3) = 2.4 \times 10^{-2} \text{ cm}^2 \text{ s}^{-1}$ and an activation energy $E_d(\beta_3)$ which varies linearly with increasing coverage from 51 to 41 kcal/mol.²

The maximum amount of O_2 desorbing from the $\beta_1 + \beta_2$ -states (which are only observed if O_{ad} is formed from NO_2) is twice as large as that from the β_3 -state, as becomes evident from numerical integration of the corresponding TDS traces. The β_1 -state starts to develop above $\theta_0 \approx 0.4$, but no attempt was made to separate it from the β_2 -state. The temperature of the maximum rate, T_{max} , of the latter state is independent of coverage at about 645 K. This effect can be interpreted in the simplest way in terms of pseudo-first-order desorption kinetics with constant kinetic parameters $\nu(\beta_2)$ and $E_d(\beta_2)$; hence¹²

$$\frac{E_d}{RT_{max}} = \ln\left(\frac{\nu}{\beta}\right) + \ln\left(\frac{T_{max}}{\ln(\nu/\beta)}\right), \quad (4)$$

where β is the heating rate. Assuming the frequently assumed values of 10^{13} s^{-1} for ν (which would correspond to $\approx 10^{-2} \text{ cm}^2 \text{ particles}^{-1} \text{ s}^{-1}$ for second-order kinetics) yields an estimate of $E_d(\beta_2) \approx 39 \text{ kcal/mol}$. This number is smaller by 2 kcal/mol than the desorption energy from the β_3 -state at $\theta = 0.25$ (41 kcal/mol, see above) which also fits the separation in temperature of about 50 K between these two states. Desorption from the β_1 -state occurs with an even lower activation energy, which is roughly estimated to be around 32 kcal/mol.

The occurrence of distinct desorption states with lower energy above $\theta_0 = 0.25$ has to be ascribed to the operation of repulsive interactions or to the occupation of different adsorption sites, but further discussion has to await structural information from LEED/HRELS studies. Preliminary LEED observations revealed that the 2×2 -pattern at $\theta_0 = 0.25$ (known from O_2 adsorption) persists up to $\theta_0 \approx 0.5$, indicating the uptake of a second O atom into the unit cell. At even higher coverages the diffraction pattern shows streak formation, indicating the onset of one-dimensional disorder.

3.3. Desorption of NO

The kinetics of desorption of NO from a Pt(111) surface either in the limit of zero coverage or in the

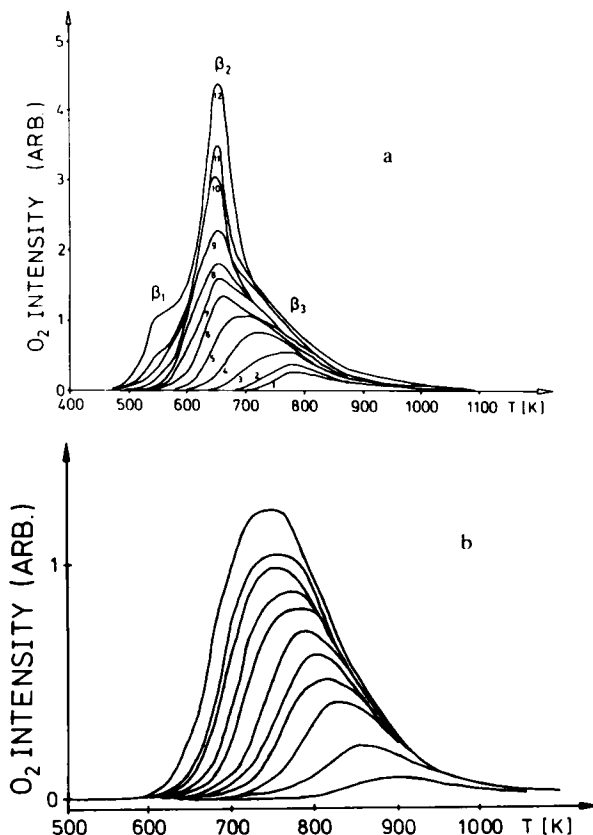


Fig. 5. Thermal desorption spectra for O_2 : (a) after NO_2 exposure at 440 K (1:0.31 L, 2:0.47 L, 3:0.62 L, 4:0.94 L, 5:1.25 L, 6:1.56 L, 7:1.87 L, 8:2.5 L, 9:3.1 L, 10:4.4 L, 11:5.6 L, 12:18.7 L [= 0.6 ML]); (b) after O_2 exposure at 517 K ($\theta_{max} = 0.25$ ML after 100 L exposure).

presence of adsorbed NO or O was studied in detail previously^{3,9} so that no essentially new information concerning this aspect could be expected from the present experiments. In brief, first-order desorption of NO from a clean Pt(111) surface is characterized by kinetic parameters $\nu = 10^{15.5} \text{ s}^{-1}$ and $E_d = 33.1 \text{ kcal/mol}$ which are lowered both by NO_{ad} and O_{ad} . At $\theta_0 = 0.25$, for example, $E_d \approx 17 \text{ kcal/mol}$ was determined.³

In the present context, however, it was of interest whether upon dissociation of NO_2 , the NO formed may be directly released into the gas phase (i.e. $NO_2 \rightarrow NO + O_{ad}$) or whether it is first chemisorbed (i.e. $NO_2 \rightarrow NO_{ad} + O_{ad}$). The data in Fig. 2 indicate, in fact, at low coverages the build-up of equal amounts of NO_{ad} and O_{ad} at 300 K. (At higher coverages the adsorption energy of NO decreases so that substantial desorption takes place even at 300 K.)

In order to investigate this point in more detail, the relaxation time τ for NO formation at higher temperatures was directly determined by means of modulated beam experiments. In these measurements the primary beam was periodically chopped with a frequency ω and the phase shift ϕ of the modulated signal from particles coming off the surface was recorded by means of lock-in techniques. Details on the proper handling of data can be found in previous papers.^{2,3} For a first-order rate process the phase lag ϕ is simply determined by

$$\tan \phi = \omega \tau \quad (5)$$

where $\tau = 1/k$ is the reciprocal of the rate constant. In the case of a simple adsorption/desorption process such as $\text{NO} \rightleftharpoons \text{NO}_{\text{ad}}$, k is equal to the rate constant for desorption and the kinetic parameters mentioned above have been determined in this way.³ In the present experiments k denotes the overall rate constant for the process $\text{NO}_2 \rightarrow \text{NO} (+\text{O}_{\text{ad}})$ since the phase lag between NO_2 impingement and NO evolution is determined.

In order to obtain data in the limit of zero coverage the measurements were performed in an atmosphere of 7×10^7 torr H_2 which readily reacts off the O_{ad} formed, and at temperatures > 540 K where NO (as well as H_2 or H_2O) desorption is so rapid that no measurable steady-state coverage could be built up under the applied beam conditions.

Data for τ ($= 1/k$) (derived from phase lag measurements at three different chopping frequencies) at various surface temperatures are reproduced in Fig. 6 in Arrhenius form, viz. $\ln k_d$ vs. $1/T$. The resulting kinetic parameters, $\nu = 10^{15.3} \text{ s}^{-1}$ and $E = 33.7 \pm 1 \text{ kcal/mol}$, are identical within the limits of error with those determined previously for the desorption of NO (see above)³ and demonstrate unequivocally: (i) NO formed by heterogeneous decomposition of NO_2 is intermediately chemisorbed; (ii) the overall rate of the process $\text{NO}_2 \rightarrow \text{NO}_{\text{ad}} (+\text{O}_{\text{ad}}) \rightarrow \text{NO}$ is determined by the rate of NO desorption.

4. DISCUSSION

Nitrogen dioxide is a bent triatomic molecule ($\text{O}-\text{N}-\text{O}$ angle 134° ¹³) having one electron more than linear CO_2 . While dissociation of the latter molecule at a clean $\text{Pt}(111)$ surface into $\text{CO}_{\text{ad}} + \text{O}_{\text{ad}}$ would require an activation energy of around 30 kcal/mol ,⁴ the corresponding

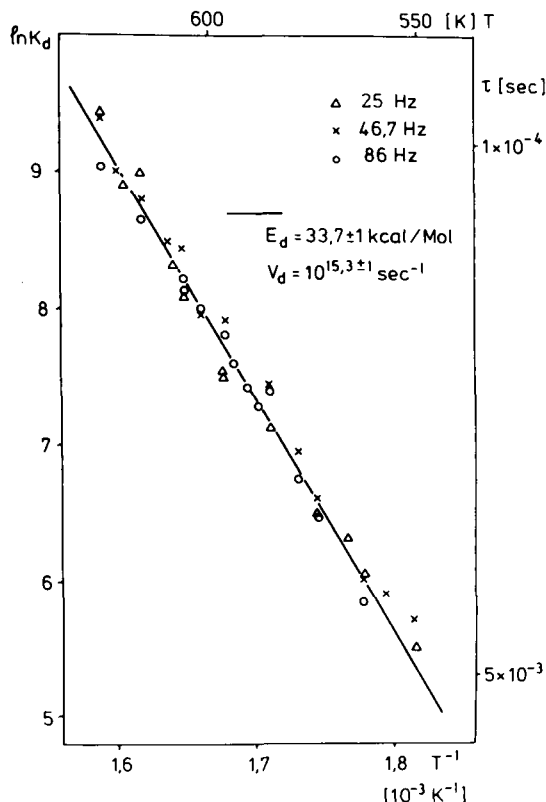
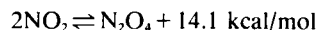


Fig. 6. Arrhenius plot of the relaxation time for NO formation (see text).

reaction with NO_2 is non-activated and occurs at room temperature with a probability of almost unity. The high reactivity of NO_2 towards transition metals has indeed been known for a long time: Sabatier and Senderens¹⁴ even observed ignition in the oxidation of nickel to NiO by NO_2 .

In fact, due to the equilibrium¹⁵



it was to be expected that an appreciable fraction of the molecules striking the surface was indeed in the form of N_2O_4 , the dimerisation processes being assisted by the adiabatic expansion in the nozzle.¹⁶ It is estimated that under the applied experimental conditions roughly about 50% of the molecules striking the surface were dimers. Qualitative confirmation was obtained from the intensity ratio of masses 46:30 within the primary beam which was considerably higher (≈ 1) than the literature value (0.37).¹⁷ This ratio decreased, on the other hand, to about 0.3 after scattering at a graphite surface which shows that interaction of N_2O_4 with a rather inert surface suffices to dissociate this molecule into monomers.

The reason why NO_2 , in contrast to CO_2 , dissociates so readily at $\text{Pt}(111)$ appears to be quite obvious: while the adsorption energies of NO and CO are quite similar,^{1,3} the energy for dissociating the $\text{O}-\text{NO}$ bond (in the free molecule) is much smaller (73 kcal/mol) than that for the $\text{O}-\text{CO}$ bond (127 kcal/mol).¹⁵ The potential diagram of Fig. 7 illustrates qualitatively the energetics of the process. The (dissociative) adsorption energy on clean $\text{Pt}(111)$, $E_{\text{ad}} = 39 \text{ kcal/mol}$, follows from the adsorption energies for NO ($E_{\text{NO}} = 27 \text{ kcal/mol}$ ¹⁸) and O_2 ($E_{\text{O}_2} = 51 \text{ kcal/mol}$ ¹⁹) from

$$E_{\text{ad}} = \frac{1}{2}(E_{\text{O}_2} + E_{\text{diss},\text{O}_2}) + E_{\text{NO}} - E_{\text{diss},\text{NO}_2}$$

where $E_{\text{diss},\text{O}_2}$ (119 kcal/mol) and $E_{\text{diss},\text{NO}_2}$ (73 kcal/mol) are the dissociation energies for O_2 and $\text{O}-\text{NO}$, respectively.

The energy for molecular adsorption of NO_2 is so far unknown due to the instantaneous dissociation of this molecule upon interaction with the surface. The high

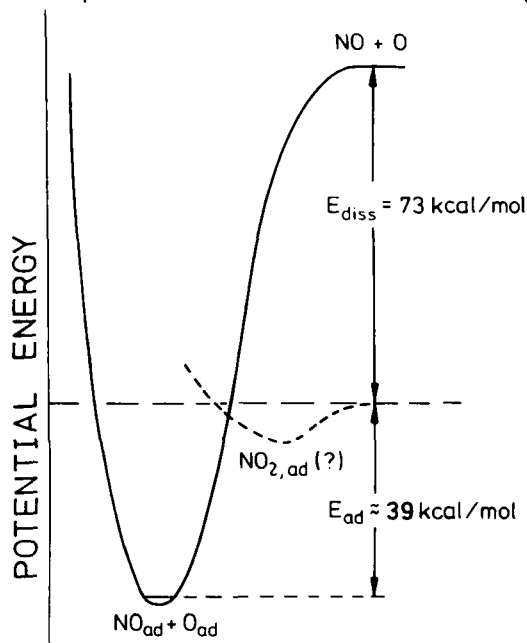


Fig. 7. Schematic potential energy diagram for NO_2 adsorption.

sticking coefficient suggests that it is considerably higher than that for CO_2 (≤ 10 kcal/mol²⁰) or O_2 (~ 8 kcal/mol^{8,21}). Bonding is presumably occurring through the N atom via the singly occupied $4a_1$ -orbital in a similar manner as in N_2O_4 .²²

While oxygen adsorption on Pt(111) has so far been believed to reach saturation at a coverage of 0.25,^{2,8,23,24} the present data demonstrate that a much higher coverage (0.75) can be achieved. The more or less continuous variation of the adsorption energy with coverage suggests the existence of chemisorbed oxygen even at higher surface concentrations, rather than the formation of subsurface or oxide species. (In fact, no evidence for the formation of oxides decomposing at temperatures above 1000 K²⁵ was found with the present experiments.) The failure to reach $\theta_0 > 0.25$ by exposure to O_2 is caused by kinetic effects. The initial sticking coefficient for O_2 on Pt(111) is of the order ~ 0.05 and drops rapidly with coverage,² so that "clean-off" reactions with spurious amounts of H_2 or CO in the background pressure may play an important role. By contrast, the sticking coefficient of NO_2 is much higher so that this gas provides a very effective source of surface oxygen. Recently, Barteau et al.²⁶ were able to produce higher oxygen coverages with the system $\text{O}_2/\text{Pt}(100)$ and the TDS data show close resemblance with the $(\beta_1 + \beta_2)$ -states observed in the present work.

The modulated beam experiments demonstrated that the heterogeneous reaction $\text{NO}_2 \rightarrow \text{NO} + \text{O}_{\text{ad}}$ proceeds via NO_{ad} , whereby desorption of NO is much slower than dissociation of NO_2 . The steady-state reaction $2\text{NO}_2 \rightarrow 2\text{NO} + \text{O}_2$ (although not studied in detail here) would be limited in rate by desorption of oxygen which (according to the TDS data) would become appreciable above about 450 K. At this temperature, on the other hand, the homogeneous reaction already proceeds²⁷ so that a Pt catalyst would be of minor assistance. The system finally reaches equilibrium, which means that the recombination $\text{NO}_{\text{ad}} + \text{O}_{\text{ad}} \rightarrow \text{NO}_2$ also takes place on the surface. The present experiments were, however, performed under conditions very far from equilibrium, so that this latter reaction was of negligible importance.

APPENDIX

Determination of the beam flux and of the O and NO coverage. According to Eq. (2), $n_s = I_0 \int_0^t s(t) dt$, the primary flux, I_0 , and the density of adsorbed particles, n_s , are connected with each other through the sticking coefficient $s(t)$ which is determined through Eq. (1), independent of any assumptions. Calibration of the oxygen coverage was achieved in the present case through the area $\int p dt$ below thermal desorption traces of desorbing O_2 and by comparison with the saturation value obtained after exposure to O_2 . In this case $\theta_0 = 0.25$ ($n_s = 3.8 \times 10^{14}$ O-atoms/cm²) is achieved, as determined previously.² Numerical integration of $\int s(t) dt$ then provided $I_0 = 2.37 \times 10^{14}$ NO_2 molecules/cm² s, corresponding to a pressure of 6.24×10^{-8} torr in the molecular beam experiments. This flux is smaller than in previous work with O_2 , CO or NO , and is caused by the reduced diffusivity of NO_2 ($+ \text{N}_2\text{O}_4$).

Once I_0 was known, n_s could in turn be determined from adsorption transients through Eq. (2). This procedure is, however, only applicable at temperatures < 450 K as long as desorption of O_2 is negligible.

Determination of the NO coverage was much more complicated. Desorption takes place already at room temperature and the $m/e = 30$ signal in the mass spectrometer is caused not only by NO but also contains contributions from the cracking of NO_2 .

If complete desorption of NO takes place (i.e., above 400 K) the intensity of $m/e = 30$ recorded, i_{30} , is given by

$$i_{30} = \alpha \cdot (1 - s(t)) \cdot I_0 + \beta \cdot s(t) I_0, \quad (6)$$

where I_0 is the primary flux of NO_2 . The first term represents the fraction of NO_2 reflected back from the surface, the proportionality factor α characterizing the contribution of NO_2 to the $m/e = 30$ signal due to cracking in the mass spectrometer. The second term is caused by the fraction of NO_2 being dissociatively adsorbed and subsequently desorbed as NO; the factor β is now related to the ionization probability of NO. By measuring i_{30} , $s(t)$ and I_0 the factors α and β could be determined.

Once α and β were known, i_{30} corresponding to complete desorption of NO could in turn be calculated through Eq. (6). At lower temperatures the measured i_{30} is, however, smaller since part of the NO formed remains adsorbed. If the corresponding transients are numerically integrated the difference from the result predicted by Eq. (6) yields the NO coverage. Checking the resulting numbers with thermal desorption data yielded deviations of less than 5% in the θ_{NO} values.

Acknowledgements. Financial support by the Deutsche Forschungsgemeinschaft (SFB 128) and by the Max Buchner Stiftung is gratefully acknowledged.

REFERENCES AND NOTES

- C. T. Campbell, G. Ertl, H. Kuipers and J. Segner, *Surf. Sci.*, **107**, 207 (1981).
- C. T. Campbell, G. Ertl, H. Kuipers and J. Segner, *Surf. Sci.*, **107**, 220 (1981).
- C. T. Campbell, G. Ertl and J. Segner, *Surf. Sci.*, **115**, 309 (1982).
- C. T. Campbell, G. Ertl, H. Kuipers and J. Segner, *J. Chem. Phys.*, **73**, 5862 (1980).
- T. Engel, *J. Chem. Phys.*, **69**, 373 (1978).
- S. Daiser and K. Wandelt, unpublished results.
- G. Ertl, *Surf. Sci.*, **89**, 525 (1979).
- J. L. Gland, *Surf. Sci.*, **93**, 487 (1980).
- R. J. Gorte, L. D. Schmidt and J. L. Gland, *Surf. Sci.*, **109**, 367 (1981).
- P. Kisluk, *J. Phys. Chem. Solids*, **5**, 78 (1958).
- D. A. King and M. G. Wells, *Proc. R. Soc. London, Ser. A*, **339**, 245 (1974).
- P. A. Redhead, *Vacuum*, **12**, 203 (1962).
- K. Hedberg, *Trans. Am. Crystallogr. Assoc.*, **2**, 79 (1966).
- P. Sabatier and J. B. Senderens, *Ann. Chim. Phys.*, **7**, 394 (1896).
- Handbook of Physics and Chemistry*, 48th Ed., p. F-154.
- F. T. Greene and T. A. Milne, *J. Chem. Phys.*, **39**, 3150 (1963).
- A. Cornu and R. Massot, *Compilation of Mass Spectra Data*, Hayden & Sons, London.
- A value of 27 kcal/mol for NO adsorption at a perfect Pt(111) surface was determined in Ref. 3. Gorte et al.⁹ obtained a value of 25 kcal/mol from their TDS data.
- This number was derived from molecular beam experiments.² There is, however, considerable scatter in the literature on the initial heat of oxygen adsorption on Pt(111).
- P. R. Norton and P. J. Richards, *Surf. Sci.*, **49**, 567 (1975).
- J. L. Gland, B. A. Sexton and G. B. Fischer, *Surf. Sci.*, **95**, 587 (1980).
- D. C. Frost, C. A. McDowell and N.P.C. Westwood, *J. Electr. Spectros. Rel. Phenom.*, **10**, 293 (1977).
- H. Hopster, H. Ibach and G. Comsa, *J. Catal.*, **46**, 37 (1977).
- D. R. Monroe and R. P. Merrill, *J. Catal.*, **65**, 461 (1980).
- T. Matsushima, D. B. Almy and J. M. White, *Surf. Sci.*, **67**, 89 (1977); C. E. Smith, J. P. Biberian and G. A. Somorjai, *J. Catal.*, **57**, 426 (1979); H. Niehus and G. Comsa, *Surf. Sci.*, **93**, 147 (1980).
- M. A. Barteau, E. I. Ko and R. J. Madix, *Surf. Sci.*, **102**, 99 (1981).
- M. Bodenstein, *Z. Phys. Chem.*, **100**, 68 (1922).